



ACADEMIC
PRESS

Available online at www.sciencedirect.com

SCIENCE @ DIRECT®

Icarus 162 (2003) 171–182

ICARUS

www.elsevier.com/locate/icarus

Photometry of Pluto in the last decade and before: evidence for volatile transport?

B.J. Buratti,^{a,*} J.K. Hillier,^{a,1} A. Heinze,^a M.D. Hicks,^a K.A. Tryka,^a J.A. Mosher,^a J. Ward,^a
M. Garske,^a J. Young,^a and J. Atienza-Rosel^b

^a *Jet Propulsion Laboratory, Palomar Observatory, California Institute of Technology, 4800 Oak Grove Drive, Mailstop 183-501, Pasadena, CA 91109, USA*

^b *Department of Physics and Astronomy, California State University—Los Angeles, Los Angeles, CA, USA*

Received 30 May 2001; revised 17 October 2002

Abstract

Photometric observations of Pluto in the BVR filter system were obtained in 1999 and in 1990–1993, and observations in the 0.89- μm methane absorption band were obtained in 2000. Our 1999 observations yield lightcurve amplitudes of 0.30 ± 0.01 , 0.26 ± 0.01 , and 0.21 ± 0.02 and geometric albedos of 0.44 ± 0.04 , 0.52 ± 0.03 , and 0.58 ± 0.02 in the B, V, and R filters, respectively. The low-albedo hemisphere of Pluto is slightly redder than the higher albedo hemisphere. A comparison of our results and those from previous epochs shows that the lightcurve of Pluto changes substantially through time. We developed a model that fully accounts for changes in the lightcurve caused by changes in the viewing geometry between the Earth, Pluto, and the Sun. We find that the observed changes in the amplitude of Pluto's lightcurve can be explained by viewing geometry rather than by volatile transport. We also discovered a measurable decrease since 1992 of ~ 0.03 magnitudes in the amplitude of Pluto's lightcurve, as the model predicts. Pluto's geometric albedo does not appear to be currently increasing, as our model predicts, although given the uncertainties in both the model and the measurements of geometric albedo, this result is not firm evidence for volatile transport. The maximum of methane-absorption lightcurve occurs near the minimum of the BVR lightcurves. This result suggests that methane is more abundant in the brightest regions of Pluto. Pluto's phase coefficient exhibits a color dependence, ranging from 0.037 ± 0.01 in the B filter to 0.032 ± 0.01 in the R filter. Pluto's phase curve is most like those of the bright, recently resurfaced satellites Triton and Europa. Although Pluto shows no strong evidence for volatile transport now (unlike Triton), it is important to continue to observe Pluto as it moves away from perihelion.

© 2003 Elsevier Science (USA). All rights reserved.

Keywords: Pluto, Surfaces, planets; Photometry

I. Introduction

The *Voyager II* spacecraft revealed that even frozen icy bodies at the edge of the Solar System exhibit active volcanism and seemingly transient condensed volatiles such as methane, nitrogen, carbon dioxide, and carbon monoxide. Several geysers and many plume-deposits were observed on Triton, the large satellite of Neptune (Smith et al., 1989). A long-term record of seasonal transport of volatiles on Triton

is provided by telescopic observations of Triton's albedo variegations and color through the historical period it has been known to astronomers (Buratti et al., 1994).

Pluto, a body similar to Triton in many ways (see Table 1), is the only planet in the Solar System that has not been scrutinized by a spacecraft. Soon after the discovery of methane ice on Pluto (Cruikshank et al., 1976), it was realized that Pluto must possess at least a tenuous atmosphere because methane has a nonzero vapor pressure at Pluto's equilibrium temperature (Cruikshank and Silvggio, 1979; Trafton, 1980). With the discovery during a stellar occultation of a significant atmosphere (Hubbard et al., 1989; Elliot et al., 2000) and the spectroscopic detection of the more abundant component ni-

* Corresponding author. Fax: +1-818-354-0966.

E-mail address: bonnie.buratti@jpl.nasa.gov (B. J. Buratti).

¹ Now at Grays Harbor College, Grays Harbor, WA.

Table 1
Physical properties of Pluto (with Triton for comparison)

	Pluto	Triton
Heliocentric distance (AU)	30–50	30
Orbital period (years)	248	165
Orbital inclination (°)	17	157 ^a
Orbital eccentricity	0.25	0.0009 ^a
Rotation period (days)	6.3872	5.88
Radius (km)	1180	1350
Bulk density	2.1	2.1
Visual geometric albedo	0.55	0.70
Atmosphere (μ bar)	3–60 ^b	14
Surface temperature (K)	40–60 ^c	38
Surface composition	CH ₄ , N ₂ , CO	CH ₄ , N ₂ , CO CO ₂ , H ₂ O
Atmospheric composition	N ₂ , CH ₄	N ₂ , CH ₄

^a With respect to Neptune.

^b See text for discussion.

^c See discussion in Stern et al. (1993).

trogen (Owen et al., 1993), a much more volatile substance with a vapor pressure on Pluto's surface 4 orders of magnitude greater than that of methane, the idea of a significant atmosphere was established. With its high eccentricity (Pluto's distance from the Sun varies from about 30 to nearly 50 AU, a change in distance that corresponds to a factor of 2.8 in insolation) and an obliquity of 122°, causing a substantial excursion in subsolar latitude, seasonal volatile transport on the planet should be significant (Trafton and Stern, 1983; Stern and Trafton, 1984; Stern et al., 1988; Trafton, 1990; Hansen and Paige, 1996). These models are based on the idea of a seasonal atmosphere caused by oscillations of several orders of magnitude in vapor pressures of the major atmospheric components. Although estimates of the surface pressure of Pluto's atmosphere range from 3 μ bars based on a model (Trafton et al., 1998) to 19 μ bars based on occultation measurements and subsequent analysis (Elliot et al., 2000) to 58 μ bars based on the N₂ frost temperature (Stansberry et al., 1994; Young, 1994) to 60 μ bars based on the line width of nitrogen (Tryka et al., 1994), the consensus is that the atmosphere is in vapor-pressure equilibrium with the surface, at least at perihelion. Is it possible that the planet's entire atmosphere is seasonal, sublimating only in the period around perihelion, and "collapsing" back onto the surface after a few decades? The evolution of Pluto's atmosphere depends so sensitively on a variety of factors, including the mixing ratios of atmospheric constituents, and the composition, albedo, and emissivity of the surface, that the various models present conflicting answers to this basic question (Stansberry et al., 1996; Trafton et al., 1998; Stansberry and Yelle 1999).

Careful photometric observations of Pluto can provide the groundwork for answering this question. Evidence for the seasonal deposition or sublimation of ice on Pluto's surface should be detectable with Earth-based telescopes. Rotational lightcurves obtained between 1954 and 1997 have increased markedly in amplitude, and concomitant decreases have occurred in the planet's geometric albedo

(see summary by Stern et al., 1988, and the recent results of Buie et al., 1997). These lightcurves can be deconvolved to provide rough albedo maps (Marcialis, 1988) as a function of epoch, once the effects of viewing geometry are modeled. More accurate albedo maps were derived from the mutual events that occurred between 1985 and 1990 (Buie et al., 1992; Young and Binzel, 1993; Young et al., 1999) and from Hubble Space Telescope (HST) images (Stern et al., 1997). The complicating factor is, of course, that the geometry with which a terrestrial observer views Pluto changes with epoch, and these changes must be fully accounted for. It is especially important to search for evidence for volatile transport at this unique time, as Pluto passes through its perihelion. Even if volatile transport is not currently occurring, accurate photometric observations will provide a baseline for comparison with future observations.

In this paper, we present three new sets of lightcurves that were obtained during the 1990s. An intensive, dedicated campaign during the summer of 1999 at Table Mountain Observatory produced lightcurves in the B, V, and R filters with good longitudinal resolution. In 2000 we obtained a methane lightcurve of Pluto at the same facility with a narrow band (0.005 μ m FWHM) 0.89- μ m methane-absorption filter. A third, more sporadic campaign conducted with the 60-in. telescope on Palomar Mountain throughout the early 1990s produced a lightcurve with less longitudinal resolution, but with good photometric accuracy. We compare our 1999 observations, along with previously published lightcurves of Pluto, with a time-dependent model lightcurve of Pluto that fully accounts for changes in viewing geometry between Pluto, the Earth, and the Sun. The model is based on HST images of Pluto (Stern et al., 1997). We find that historical changes in the lightcurve of Pluto can be most easily explained by the effects of viewing geometry, rather than by volatile transport.

In addition to detecting the seasonal transport of volatiles on Pluto, a current lightcurve of Pluto is required as background for understanding whether there is a nonzero eccentricity in Charon's orbit (Null et al., 1993; Tholen and Buie, 1997). The determination of the orbit of the Pluto–Charon system depends on centroiding each object accurately, which depends in turn upon the albedo distribution on the object's disk at the time of the observation. Finally, changes in Pluto's lightcurve could offer evidence for active geologic processes on the planet.

It is important to remember that the historical lightcurves of Pluto, as well as the new lightcurves obtained at Table Mountain Observatory, are actually measurements of the Pluto–Charon system. Pluto contains 84% of the visible light of the system (Buie et al., 1997). Although our derived geometric albedos are for Pluto alone, the signal from Charon has not been subtracted from the lightcurves of Pluto, in order to facilitate comparisons with earlier epochs. The one measured lightcurve of Charon exhibits an amplitude of at most 0.07 mag, only a fourth of Pluto's (Buie et al., 1997). Thus, at least 96% of the measured lightcurve amplitude of the system is due to Pluto, at least during the current epoch.

Table 2
Summary of Table Mountain Observations, 1999

Time (UT)	No. images			θ	α	r	D
	B	V	R				
1999:							
June 6 04:44–11:40	8	7	9	212–229	0.44	30.163	29.175
7 04:32–11:36	7	6	7	268–284	0.46	30.164	29.177
8 04:05–11:20	9	8	8	323–340	0.47	30.164	29.179
9 03:57–11:26	7	8	13	19–37	0.49	30.164	29.182
18 04:11–10:24	7	7	8	167–182	0.70	30.167	29.218
19 04:01–10:39	8	8	9	223–238	0.72	30.167	29.224
20 04:14–10:45	8	8	9	280–295	0.75	30.167	29.229
21 04:13–10:42	8	8	8	336–351	0.77	30.167	29.235
22 04:37–10:21	8	12	10	33–47	0.80	30.168	29.241
23 04:23–10:14	8	10	6	89–103	0.83	30.168	29.248
July 14 05:09–08:49	3	6	2	194–202	1.35	30.174	29.441
15 04:11–08:46	6	7	7	249–259	1.37	30.174	29.452
16 04:06–08:49	6	6	6	305–316	1.39	30.174	29.465
17 05:43–08:34	7	5	4	5–12	1.41	30.175	29.477
18 04:28–08:32	6	6	6	58–68	1.43	30.175	29.489
31 04:24–07:42	8	7	8	71–79	1.67	30.179	29.665
Aug 1 04:01–07:33	8	8	7	126–134	1.69	30.179	29.680
2 03:53–07:26	10	8	8	183–191	1.70	30.179	29.695
3 03:51–07:25	8	5	5	239–247	1.72	30.179	29.710
4 04:00–07:23	11	7	7	296–304	1.73	30.180	29.725
5 03:50–07:19	7	7	6	349–359	1.74	30.180	29.740
6 03:40–07:17	10	6	5	48–56	1.76	30.180	29.755
7 03:45–07:14	8	7	6	104–112	1.77	30.181	29.770
8 03:45–07:05	8	7	5	160–168	1.78	30.181	29.785
2000 (methane filter only):							
July 22 04:33–04:46		2		25	1.47	30.285	29.624
23 03:54–04:07		2		80	1.49	30.285	29.637
24 05:32	1			140	1.51	30.285	29.651
25 04:28–05:07		2		194–195	1.53	30.286	29.664
26 03:44–04:38		3		248–251	1.55	30.286	29.677
27 03:42–04:33		2		304–306	1.56	30.286	29.691
28 04:54–05:23		2		4–5	1.58	30.287	29.705

II. Observations and data analysis

1. Table Mountain Observatory (TMO)

As part of a dedicated program, 24 nights of photometric measurements of Pluto were obtained in the BVR filter system at JPL's Table Mountain Observatory in Wrightwood, California during its opposition in the summer of 1999. The observations were obtained on a 24-in. reflecting telescope with a 1024 square CCD camera covering a field of 10 arcmin at the Cassegrain focus. Nominal integration times were 10 min. for the B filter, and 5 min. for the V and R filters. Bias frames and flatfield images in each filter were obtained at the beginning of the night. The flatfields were 1-s exposures of the inside of the dome flooded with incandescent light. Five stars in Landolt field PG1633 were observed at least three times each night as absolute photometric standards (Landolt, 1992). In 2000, 7 nights of observations in a narrow band 0.89- μm methane-absorption filter were obtained with the same observing protocol and 10-min. integration times (Landolt magnitudes were ob-

tained by interpolating between the R and I filters). The images obtained are summarized in Table 2, where θ is the west (IAU) longitude (corrected for light travel time, although the times listed in the table are Earth-received times), α is the solar phase angle, r is the Pluto–Sun distance, and D is the Pluto–Earth distance.

2. Palomar Mountain Observatory

More sporadic observations of Pluto's lightcurve were obtained with the 60-in. telescope at Palomar Mountain Observatory in the early 1990s, as time became available on our other observing programs. These observations were obtained in the B, V, and R filters with a 1024 square CCD camera covering a field of 9.6 arcmin at the Cassegrain focus. Typical integration times were 5 min. for the B filter, and 40 to 60 s for the V and R filters. Bias frames and flatfield images in each filter were obtained at the beginning of the night. The flatfields were obtained by coadding and averaging 10 images of the inside of the dome illuminated with incandescent light. One or two Landolt fields were

Table 3
Summary of Palomar Observations, 1990–1993

Time (UT)	No. images			θ	α	r	D
	B	V	R				
1990 June 19 06:30–08:36		17		353–358	1.38	29.659	28.929
1992 Jan 11 13:30–13:59	2	3	2	155–157	1.63	29.688	30.177
12 13:27–14:02		2	4	211–213	1.65	29.688	30.163
13 13:07–13:55	4		4	267–269	1.66	29.688	30.148
14 13:27–13:58		2	5	325–326	1.68	29.688	30.134
15 13:23–13:53		2	4	21–22	1.69	29.688	30.119
16 12:46–13:51		3	5	76–79	1.71	29.688	30.104
March 18 10:45–12:10		2	16	326–333	1.60	29.693	29.126
19 10:10–11:12		3	5	20–23	1.58	29.693	29.112
1993 March 3 11:30–13:17		9	8	56–259	1.83	29.725	29.423
4 10:43–13:01		10	7	311–316	1.82	29.725	29.407
5 11:34–12:34		3	3	8–10	1.81	29.726	29.391
6 08:15–13:16		15	10	57–69	1.80	29.726	29.376

observed throughout the night as absolute photometric standards. The observations are summarized in Table 3.

Each image was processed with standard routines from the IRAF software package. The bias frame was subtracted from each image and the flatfield images, and each image was then flatfielded. Relative photometry was obtained from image-to-image and from night-to-night by calculating the ratio of Pluto's sky-subtracted integral brightness to that of several (typically three to five) on-chip standard stars. Ratios of each star to the others were also checked for constancy, to confirm that none of the on-chip standard stars were variable. Because Pluto's movement from night to night was generally less than an arcminute each night, the same on-chip standards could be used for more than one night. Of course, the same standards could not usually be used for an entire observing run, but at least two standards were carried from night to night to assure an accurate relative lightcurve. Absolute photometry was accomplished by computing the magnitude of Pluto with respect to the stars in a Landolt field on the most photometric night, and tying the rest of the lightcurve to that point. In 1999, Pluto's entire 6.4-day rotational phase curve was covered several times to minimize gaps in longitudinal coverage. In the early 1990s when the coverage was more haphazard, there are significant gaps in the longitudinal coverage.

Table 4
Fourier coefficients of lightcurve

n	B filter		V filter		R filter	
	a_n	b_n	a_n	b_n	a_n	b_n
0	16.049	—	15.216	—	14.652	—
1	−0.108	0.0309	0.100	0.029	−0.089	0.026
2	0.046	−0.026	0.041	−0.026	0.038	−0.026
3	−0.003	0.007	−0.004	0.007	−0.003	0.007
4	0.000	0.006	0.004	0.003	0.001	0.002
5	0.004	−0.005	0.004	−0.007	0.005	−0.005

Errors: the 1 σ error for the leading coefficient is 0.0008 and 0.001 for the higher order coefficients.

The universal times of each observation were all corrected for light-travel time to ascertain the subobserver longitude. Each magnitude was corrected to the mean opposition distance between Pluto and the Earth (38.5 AU), and Pluto and the Sun (39.5 AU). For our TMO data, each set of observations was then fitted with a regression program to the equation

$$\text{mag}(\theta, \alpha) = \sum (a_n \cos n\theta + b_n \sin n\theta) + \beta\alpha, \quad (1)$$

where θ is the subobserver (west, in the IAU convention) geographical longitude on Pluto at the time of each observation (from JPL's Horizon's program at <http://ssd.jpl.nasa.gov/horizons.html>, which uses a rotation period of 6.38723, in close agreement with the value of 6.38726 ± 0.00007 of Tholen and Tedesco, 1994), α is the solar phase angle, a_n and b_n are the Fourier coefficients, and β is the linear phase coefficient. The coefficients for a 5th-order Fourier fit and the phase coefficients are listed in Tables 4 and 5. Our values for the phase coefficient are in good agreement with both the previous results of 0.037 ± 0.002 for the B-filter (Tholen and Tedesco, 1994) and 0.039 ± 0.002 for the V-filter (Buie et al., 1997, corrected for the entire system by weighting the individual phase coefficients by the relative brightnesses of the two components). We show for the first time that there is a clear wavelength dependence to Pluto's phase coefficient (see Section V). The excursion in phase angle from Palomar was not sufficient— 0.4° —for the determination of a solar phase curve; to correct that data we used the phase coefficients derived from our TMO model.

Table 5
Phase coefficients

Wavelength	β (mag $^\circ$)
B (0.44 μm)	0.037 ± 0.001
V (0.55 μm)	0.032 ± 0.001
R (0.68 μm)	0.032 ± 0.001

Table 6
Opposition magnitudes, geometric albedos, and lightcurve amplitudes of Pluto

	1999			1990–1993		
	Opp. mag	P^a	Amplitude	Opp. mag.	P^a	Amplitude
B	16.05 ± 0.03	0.44 ± 0.04	0.30 ± 0.01	16.15 ± 0.05	0.40 ± 0.05	0.40 ± 0.08
V	15.22 ± 0.02	0.52 ± 0.03	0.26 ± 0.01	15.20 ± 0.03	0.53 ± 0.04	0.29 ± 0.03
R	14.65 ± 0.01	0.58 ± 0.03	0.21 ± 0.02	14.65 ± 0.02	0.58 ± 0.04	0.28 ± 0.03

^a Pluto only.

Tholen and Tedesco (1994) and Binzel and Mulholland (1984) noted both secular “fading” in the brightness of Pluto. We noticed no such changes; in fact the geometric albedo of Pluto was constant for the period we observed, at least within our errors (see Table 6). We typically use one or two Landolt fields each night, with 3–10 stars in each field, so changes in a standard star would stand out as a major inconsistency. The question of Pluto’s albedo and color through time is discussed in detail in the next section.

III. Results

The resulting lightcurves for the B, V, R, and methane filters based on our TMO and Palomar observations are shown in Fig. 1. Clearly the Palomar observations are deficient when compared with those of TMO. We show the Palomar observations to establish the following: (1) the

albedo and color (B–V) of Pluto and the shape of its lightcurve did not change in the 1990–1999 period, at least within the accuracy of our measurements; and (2) the color-dependent amplitude of the lightcurve is obvious in the 1990–1993 observations (see Table 6). Because our 1999 observations agree in all essential measures with the 1990–1993 data, and because the completeness of the Palomar data is inferior to that of the TMO data, we will consider the TMO measurements our prime data set in modeling.

From our results the following can be derived:

1. Geometric albedos at B, V, and R wavelengths
2. Colors
3. Color variegations in the light curve
4. Lightcurve amplitudes, which can be compared with previous years for the purpose of detecting volatile transport
5. Phase coefficients as a function of wavelength
6. The distribution of methane on Pluto’s surface.

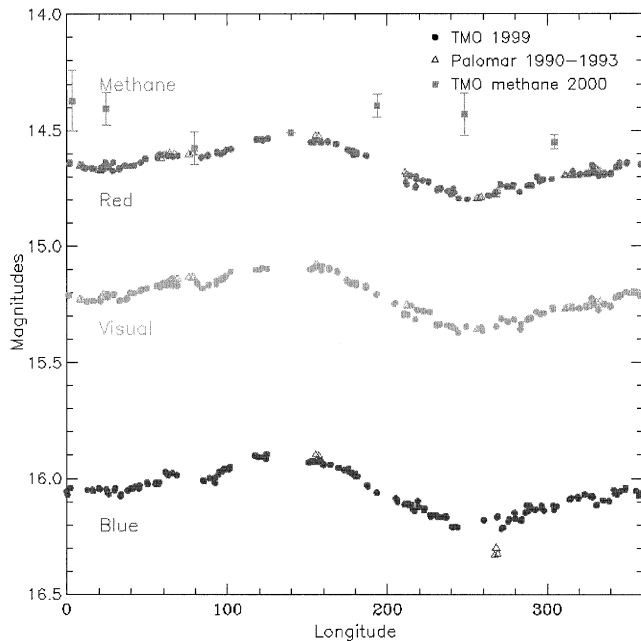


Fig. 1. The rotational lightcurves of Pluto–Charon derived from our Table Mountain and Palomar Mountain Observations. All measurements are mean opposition magnitudes. From the top, the methane ($0.89 \mu\text{m}$ absorption band), R, V, and B filters. The error bars are approximately the size of the data points, except for the methane filter, which has individual error bars depicted.

1. Geometric albedos

Geometric albedos were derived with the formula (following Horak, 1950)

$$m_{\text{pl}} - m_{\text{sun}} = -2.5 \log_{10} p - 2.5 \log_{10} [(R \cdot \rho)^2 / (r \cdot \Delta)^2], \quad (2)$$

where m_{pl} is the mean opposition magnitude of the planet, m_{sun} is the magnitude of the sun at the same wavelength, p is the geometric albedo, R is the semimajor axis of the Earth (1 AU), ρ is the planet’s radius (Table 1), r is the semimajor axis of Pluto (39.5 AU), and Δ is the distance between Pluto and the Earth at opposition (38.5 AU). In order to separate the brightness of Charon from that of Pluto, we use the V-magnitude difference between the two bodies of 1.888 mag from Buie et al. (1997) and the BVR color differences from Marcialis et al. (1993). We used the following solar magnitudes: $V = -26.75$ (Colina, 1996), $R = -27.29$ (Davies et al., 1998), and $B = -26.09$ (from the B–V in Allen, 1976). Our results are listed in Table 6, along with the opposition magnitudes and amplitudes of the lightcurves (these latter two quantities are for the Pluto–Charon system, while the geometric albedos are for Pluto only). Our observations show that throughout the 1990s the absolute albedo

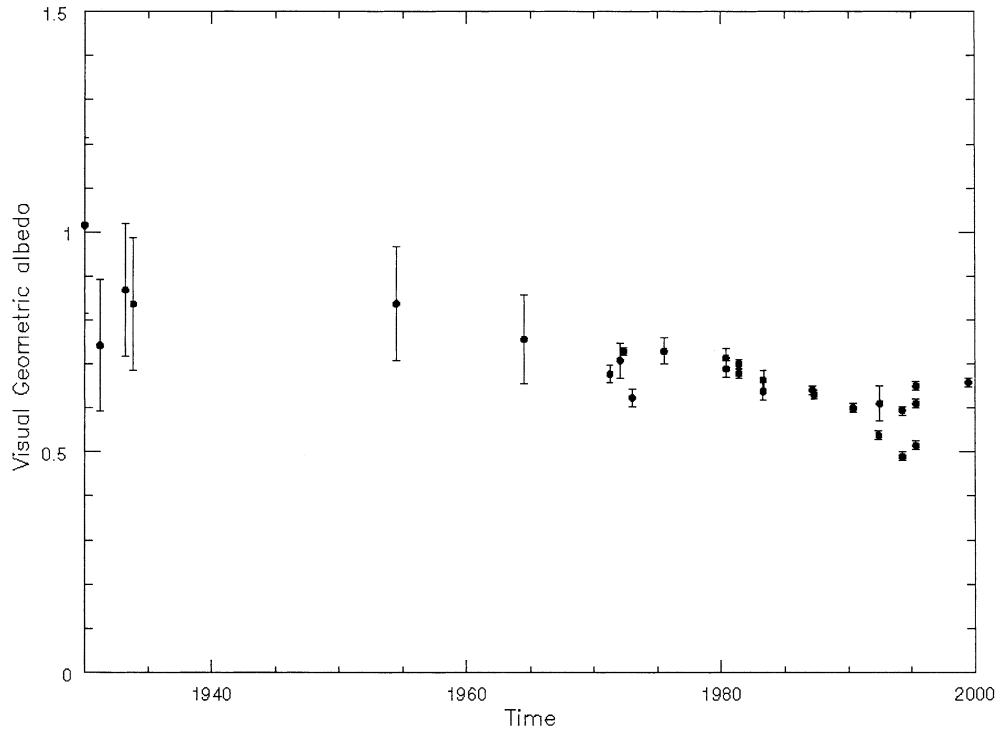


Fig. 2. The visual geometric albedo of Pluto through time, based on the observations listed in Table 7.

of Pluto has not changed to within our errors of measurement.

Purported secular changes in Pluto's albedo have caused much confusion. The albedo should change, even in the absence of volatile transport, as regions of high or low albedo move into the view of a terrestrial observer. To further investigate the existence of secular changes in Pluto's brightness, we researched all the published visual magnitudes and B–V colors of Pluto since 1930. From the magnitudes we derived geometric albedos. Often exact dates and times of the observations are not available, or it is not stated which corrections were made; further confounding our attempt to compare observations is the difference in photometric systems and overall observational integrity through the decades. Nevertheless, our "best-effort" results are shown in Fig. 2 and listed in Table 7. Qualitatively, the trend makes sense: Pluto has bright caps at both poles (Buie et al., 1992; Young and Binzel, 1993; Stern et al., 1997), so as the planet moved through a subobserver latitude of 0° in 1987 (during the peak of the eclipse season), its albedo should have reached a minimum, as Fig. 2 suggests. However, our model (Section IV) predicts an increasing albedo (at least in the B filter) since 1950. Given the low fidelity of photometric systems prior to 1980 and the fact that early observations included the brightness of Charon, we conclude that the combined measurements show no solid trend. Although our observations show no decrease in albedo between 1993 and 1999 within the 3–4% absolute accuracy of our measurements, the composite data set (Fig. 2) shows a $\sim 1\%$ decrease per year in albedo. Tholen and Tedesco

(1994) reported a secular decrease in Pluto's brightness of about 0.2% each year, which they call "fading." Continued observations with high photometric integrity should reveal a future increase in the albedo of Pluto, as our model predicts.

2. The color of Pluto

Because color is a relative quantity, it is possible to more accurately measure it than albedo. The available observations, summarized in Table 7, show that the color of Pluto has been essentially constant through time, to within the errors of the various measurements, with a B–V of 0.82 ± 0.03 .

3. Color variegations in the light curve

A color dependence to the lightcurve of Pluto means that one hemisphere should be a different color than the other. Fig. 3 is a B–R (three point average) lightcurve of Pluto, clearly showing that the trailing hemisphere, which is 25–30% darker than the leading hemisphere at visual wavelengths, is about 4% redder, as measured by B–R. This result is consistent with the findings of Buie et al. (1997), who found a B–V for the lower-albedo hemisphere of 0.873, compared to 0.862 for the higher-albedo hemisphere. Although our results are for the Pluto–Charon system, and Buie et al.'s results are for Pluto alone, the comparison is essentially valid, given the much smaller amplitude of Charon's lightcurve and its relative dimness. Marcialis and

Table 7
Published visual geometric albedos and B–V of Pluto

Year	Latitude ^a	p	Error	B–V	Reference
1930.000	53	1.0	0.20		Andersson (1974)
1931.219	52	0.74	0.15		Andersson (1974)
1933.214	53	0.87	0.15		Andersson (1974)
1933.833	55	0.84	0.15		Whyte (1980)
1954.5	54	0.84	0.13		Whyte (1980)
1964.5	44	0.76	0.10		Whyte (1980)
1971.247	33	0.68	0.02		Andersson and Fix (1973)
1972.038	30	0.71	0.04		Andersson and Fix (1973)
1972.351	31	0.73	0.01		Andersson and Fix (1973)
1972.5			0.82		Andersson (1974)
1973.008	28	0.62	0.02		Andersson et al. (1983)
1975.5	27	0.73	0.03		Marcialis (1988)
1980.375	16	0.71	0.02	0.80	Lyutyi and Tarashchuk (1982, 1984)
1980.375	16	0.69	0.02		Lyutyi and Tarashchuk (1982, 1984)
1981.408	14	0.70	0.01		Lyutyi and Tarashchuk (1982, 1984)
1981.408	14	0.68	0.01		Lyutyi and Tarashchuk (1982, 1984)
1983.296	9	0.64	0.02		Grundy and Fink (1996)
1983.299	9	0.66	0.02		Grundy and Fink (1996)
1987.170	0	0.64	0.01	0.86	Marcialis et al. (1993)
1987.310	1	0.63	0.01		Doute et al. (1999)
1989.493	–2			0.82	Blanco et al. (1994)
1990.389	–5	0.60	0.01		Grundy and Fink (1996)
1990.490	–5			0.82	Blanco et al. (1994)
1992.403	–9	0.54	0.01		Doute et al. (1999)
1992.5	–10	0.52	0.04	0.85 ± 0.06	This study
1992–1993	–10	0.61		0.86–0.87	Buie et al. (1997)
1994.287	–14	0.59	0.01		Grundy and Fink (1996)
1994.290	–14	0.49	0.01		Doute et al. (1999)
1995.359	–16	0.52	0.01		Doute et al. (1999)
1995.364	–16	0.61	0.01		Doute et al. (1999)
1995.370	–16	0.65	0.01		Doute et al. (1999)
1999.5	–23	0.52	0.03	0.85 ± 0.03	This study

^a IAU convention.

Lebofsky (1991) also showed that the lowest albedo material on Pluto is the reddest.

4. Pluto's lightcurve through time

The shape and amplitude of a planet's lightcurve is a rough measure of the distribution of high- and low-albedo regions on its surface (if one assumes sphericity). Changes in the lightcurve through time are thus key indicators of volatile transport or large-scale active geologic processes, if one corrects for the effects of viewing geometry. Fig. 4 is a comparison of our observations in the B filter with those of Tholen and Tedesco almost 20 years earlier. Clearly there are changes in the shape of the lightcurve. Fig. 5 is a comparison of the earlier V-filter lightcurves with ours at approximately 10-year intervals (the curves are normalized to the highest albedo). Even with the poor photometric quality of rotational lightcurves prior to 1980, it is easy to see that the amplitude of Pluto's lightcurve has substantially increased over the past 50 years.

5. Phase coefficients as a function of wavelength

Our 1999 observations enabled the first determination of the wavelength dependence of Pluto's phase coefficient (Table 5). Fig. 6 shows the phase curve of Pluto in each of three filters, with each best-fit linear phase curve derived from Eq. (1). The results show an inverse relationship between the wavelength and the corresponding phase coefficient, a correlation that has been noted for many other objects and even among objects (e.g., Noland et al., 1974; Millis and Thompson, 1975; Buratti and Veverka, 1983; Buie et al., 1997). The explanation for this effect depends on the relative importance of multiple scattering as the albedo of the surface increases. If one neglects the effects of coherent backscatter, the most significant physical factor in an object's phase coefficient is the compaction state of the surface (e.g., Veverka, 1977). As a body becomes fully illuminated to an observer, the rapid disappearance of mutual shadows cast by particles comprising the regolith

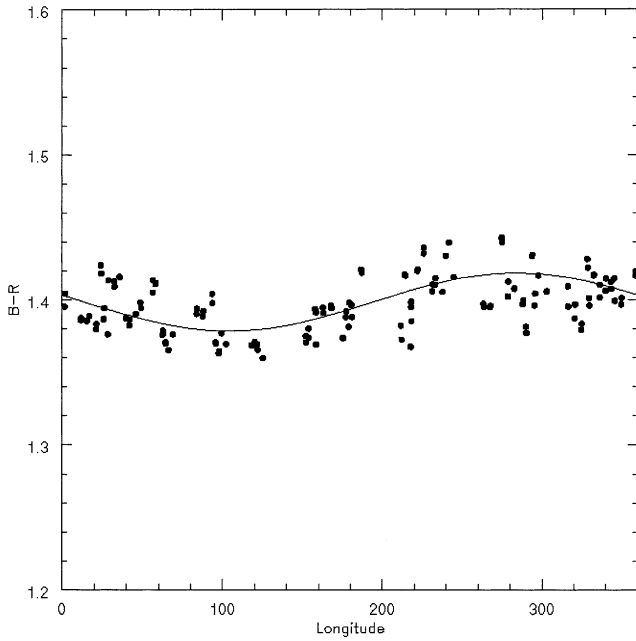


Fig. 3. The B magnitude – the R magnitude as a function of longitude. This graph shows that the low-albedo hemisphere of Pluto (180° to 360°) is slightly redder than the brighter hemisphere. The data points are three-point averages of the observations shown in Fig. 1.

causes the brightness of the object to increase far more rapidly than predicted by simple geometric scattering. As an object's albedo increases (as Pluto's does with wavelength), partial illumination of these shadows by multiply scattered

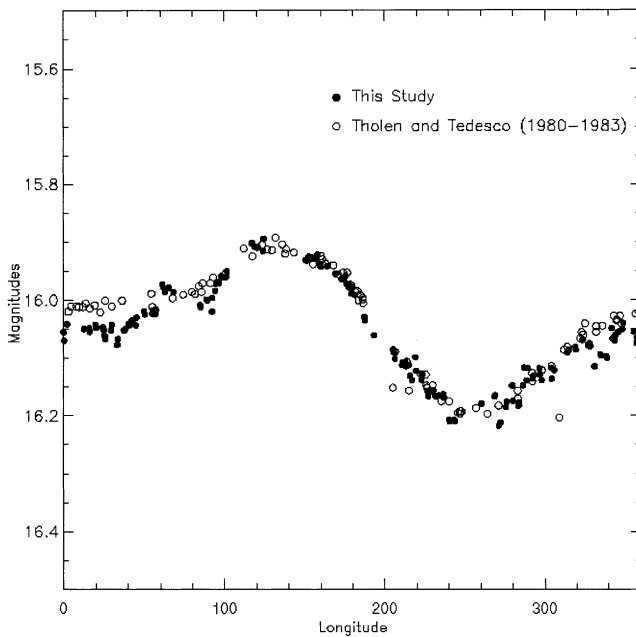


Fig. 4. A comparison of our B-filter lightcurve with that obtained 16 years earlier by Tholen and Tedesco (1994). The data are normalized to the peak brightness of the 1999 lightcurve. A significant change in the shape of the lightcurve has occurred.

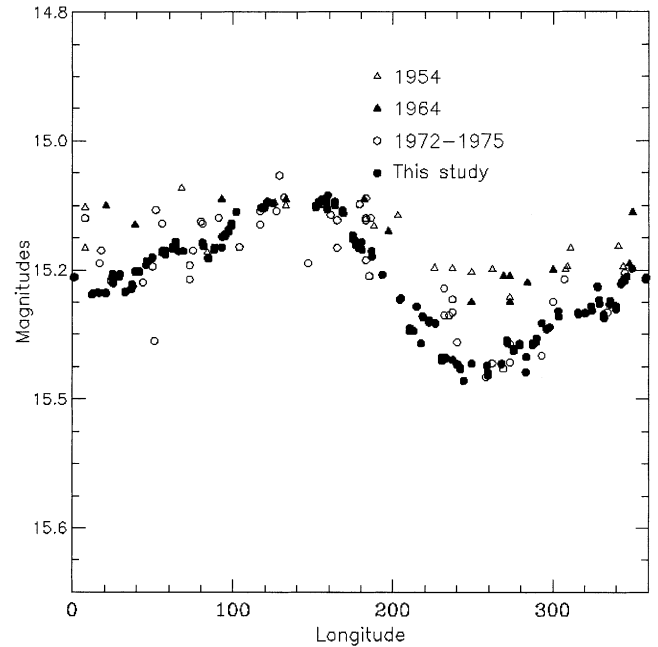


Fig. 5. A comparison of our V-filter lightcurve with those obtained earlier. The amplitude of Pluto–Charon's lightcurve has been significantly increasing with time.

photons causes the brightness of the body to decrease more slowly. A comparison of Pluto's phase curve with that of other planets and satellites is discussed in Section V.

6. The methane distribution on Pluto

The magnitude of the methane lightcurve shown in Fig. 1 is inversely proportional to the amount of methane on Pluto's surface, as the $0.89\text{-}\mu\text{m}$ filter is in the middle of an absorption band. The inverse correlation of the methane lightcurve with the brightness, at least in a rough sense, shows that the brightest regions on Pluto are methane-rich. This result is in agreement with that obtained with high-resolution visual spectroscopy 17 years earlier (Buie and Fink, 1987), with a 1988 near-infrared study (Marcialis and Lebofsky, 1991), and with a more recent near-infrared study (Grundy and Buie, 2001).

IV. A model for Pluto's lightcurve

It is clear from the measurements described in the last section that Pluto exhibits substantial changes in its lightcurve that could be attributed to seasonal volatile transport. However, the large obliquity (122°) and inclination (17°) that are responsible—along with its high orbital eccentricity—for the movement of volatiles on its surface also cause the geographic region viewed by a terrestrial observer to change significantly. HST images (Stern et al., 1997) and mutual event maps (Young et al., 1999) and ground-based light-

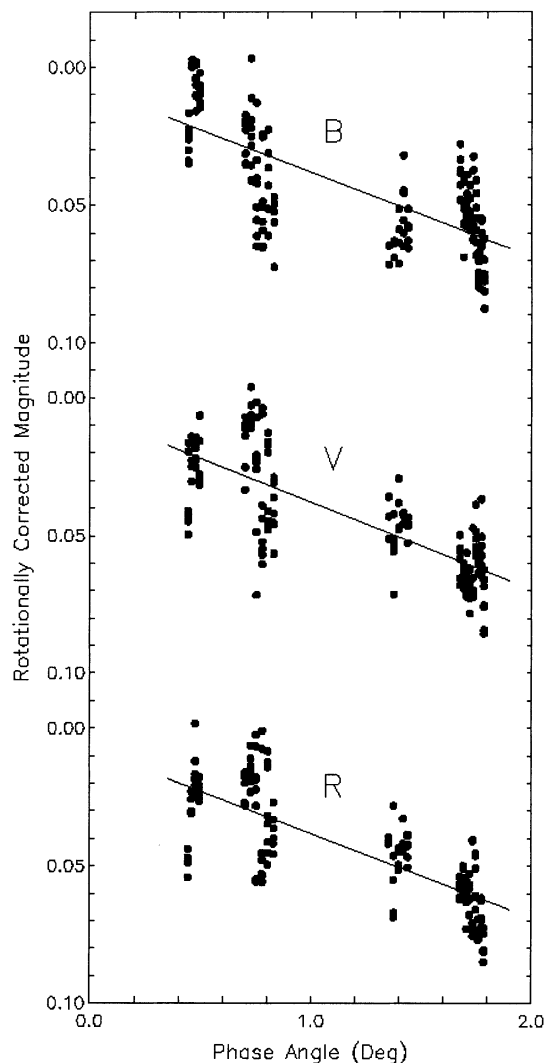


Fig. 6. The solar phase curve of Pluto–Charon in the B, V, and R filters. The points are corrected to the mean distance between the Sun, Earth, and Pluto, and for rotational effects. The line is the best-fit linear phase coefficient.

curves all show that Pluto has substantial albedo variations. As albedo features move in or out of a terrestrial observer’s point of view, significant changes in Pluto’s lightcurve will occur. In order to isolate changes in Pluto’s lightcurve due to volatile transport, it is essential to first model changes in the lightcurve expected from viewing geometry alone.

With a map of normal reflectance the lightcurve of a planet or satellite can be predicted. Further, assuming the surface does not change, we can predict how the lightcurve is expected to vary in time as a function of the varying viewing and illumination geometry. To produce these predictions, we used the maps generated by Stern et al. (1997) from HST observations that are available on the world wide web at <http://opposite.stsci.edu/pubinfo/gif/PlutoMap.gif>. The observations for this map were taken through the HST FOC F410M filter with an effective wavelength of $0.41 \mu\text{m}$.

Our procedure for generating the lightcurves is as follows. We first assumed that the phase angle was 0° (and thus the subsolar and subobserver point are the same). The geometric albedo for a given subsolar/observer latitude and longitude was determined as follows. First, we found all of the pixels that would be visible for a given subsolar/observer latitude and longitude, i.e., all the locations within 90° of the subobserver point as determined by locations where the dot product between the vector pointing to the subobserver point and that pointing to the location in question is positive. Then the normal reflectance of all the visible pixels was averaged together weighted by the cosine of the latitude (to account for distortions due to the map projection) and the cosine of the incidence angle (to account for foreshortening effects) to yield the predicted geometric albedo. The possibility of limb darkening was included in our model. However, the results shown assume no limb darkening. This assumption was made because Young and Binzel (1994) and Buie et al. (1997) found that limb darkening is not strong on Pluto and thus Stern et al. (1997) did not include limb darkening in the generation of the HST maps we used. A lightcurve for a given subsolar/observer latitude (corresponding to a given epoch) is then generated by calculating the geometric albedo while varying the longitude through a full orbit.

The results for approximately 20-year intervals are shown in Fig. 7, along with the time-matched observations. Because the HST maps are all in east longitudes (unlike the IAU and our own convention), our synthetic curves are shown with this convention.

V. Discussion and conclusions

1. Volatile transport on Pluto

Our lightcurve from 1999 shows a significantly higher amplitude than those of previous years; in general the amplitude has been increasing with time. Fig. 7 shows that the model lightcurve of Pluto is also increasing with time due to the emergence of bright regions such as polar caps into a terrestrial observer’s line of sight. To quantify the comparison between the two sets of lightcurves, we show the predicted amplitude vs the measured amplitude through time in Fig. 8. Before 1980 V-filter measurements are plotted, and after 1980, B-filter data are plotted, to correspond to the HST wavelength (there are no B-filter lightcurves prior to 1980). The exception is the data from 1992, as there are no photometrically accurate published lightcurves in the B filter for that time frame (our B-filter lightcurve from this period contains essentially only two points). Instead we use the amplitude of the V filter (Buie et al., 1997, and Table 6).

The agreement between the predicted lightcurves, based on changes in viewing geometry, and the measured lightcurves is remarkable. Based on these results, all the changes in Pluto’s lightcurve during the past 50 years can be ac-

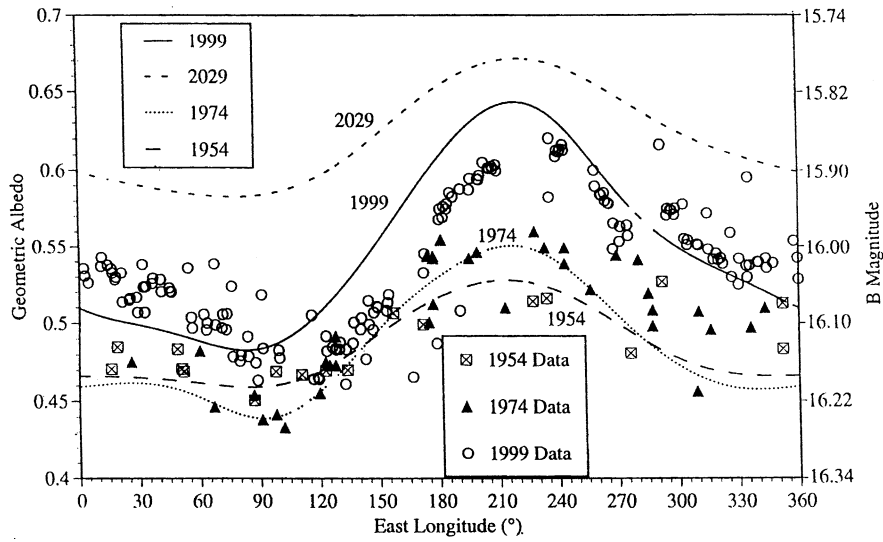


Fig. 7. A comparison of our lightcurve model with time-matched measurements of Pluto–Charon’s lightcurve obtained during the past 5 decades. The lightcurve model is based on HST maps (Stern et al., 1997), transformed to the correct viewing geometry.

counted for by viewing geometry rather than by volatile transport.

One inconsistency between the viewing-geometry model and the observations between 1950 and 2000 is that the geometric albedo is not increasing as the model predicts (Fig. 7). The subobserver latitude as seen from Earth was 54° in 1954, when the first observations of the lightcurve were obtained, 0° in 1988, and -26° in 2000 (latitudes are

in the IAU convention, where $+90^\circ$ is the rotational south pole). The predictions of our model are for a roughly constant geometric albedo between 1950 and 1975, and a slow increase after that. The trend continues to be downward or constant, which has also been noted by Tholen and Tedesco (1994) and Buie (2002). Given the difficulties in measuring geometric albedo, an absolute quantity, we do not take this finding as firm evidence for volatile transport (e.g., the

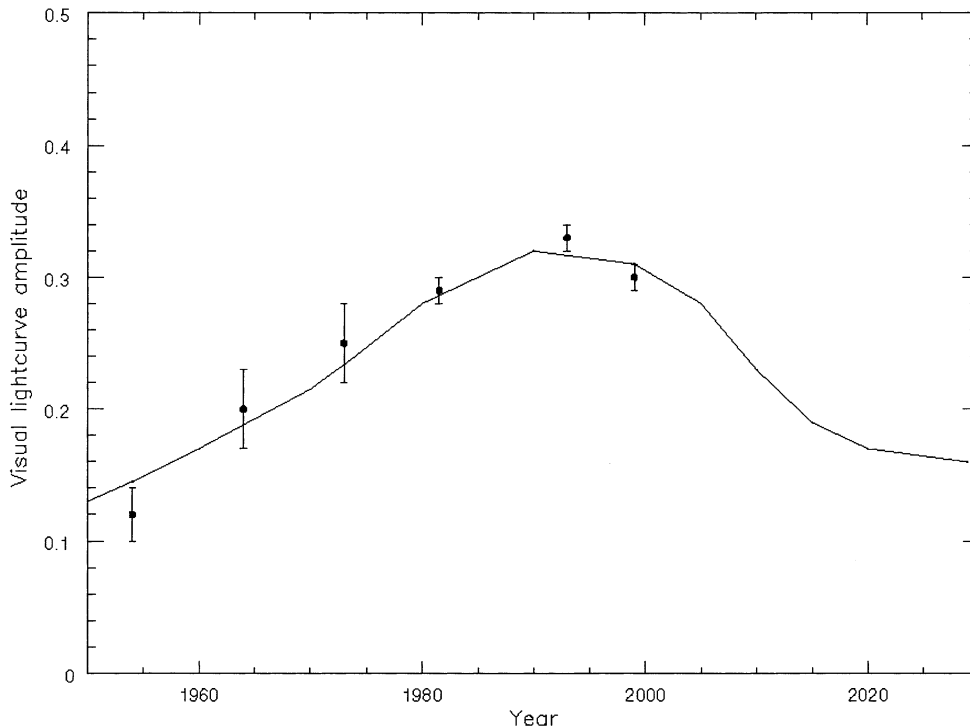


Fig. 8. A comparison of the measured amplitude of the lightcurve of the Pluto–Charon system (dots) with the predictions of our model based on the HST map (line).

denuding of a polar cap). In addition, the north polar cap of Pluto (IAU convention) was not well observed during the period the HST maps were made, so the albedo of this region may be substantially different from that depicted on the maps. Finally, high-albedo material exhibits more extreme limb-darkening than low-albedo material, with a critical change occurring in the 0.5 to 0.6 region (Buratti, 1984). Thus the albedo of Pluto's polar caps may be substantially underestimated in the HST maps. Our model predicts an increase in the geometric albedo of Pluto during the next 30 years of a dramatic 18%, a value that should easily be detectable with current ground-based photometric techniques.

It is important to monitor Pluto now as it moves away from perihelion, because this is the critical time for the possible collapse of its atmosphere onto the surface. Accurate photometric observations at the current epoch are important, as they will provide a baseline for the investigation of the subsequent condensation of methane and nitrogen onto Pluto's surface.

Fig. 8 also shows that the amplitude of Pluto's lightcurve should have reached a plateau around 1990, and then started to decrease. Our data show this effect, particularly if one compares the V data from the early 1990s and the TMO measurement. Both Buie et al. (1997) and our results yield a value of 0.29 for Pluto's V-filter lightcurve in 1992, with Buie et al.'s data giving a better constrained error of 0.01 mag. In 1999, the measured V-filter amplitude of the lightcurve is 0.26 ± 0.01 (see Table 6). Again, this change in Pluto's lightcurve is not evidence for volatile transport; on the contrary it is entirely consistent with the predicted changes in viewing geometry between the Earth, Pluto, and the Sun. Clearly, this result needs to be confirmed by future observations.

2. Pluto's phase curve

Essentially all atmosphereless bodies in the Solar System exhibit a nonlinear increase in brightness as their surfaces become fully illuminated to the observer. This effect is caused by the disappearance of mutual shadows cast among particles comprising the upper regolith. The additional effect of coherent backscatter, first discussed in the context of planetary surfaces by Hapke (1990), causes an even sharper increase in the observed brightness at very small phase angles (often $< 1^\circ$). When compared with the phase curves of other bodies, Pluto's phase curve is most like those of the bright, recently resurfaced satellites Triton and Europa (Fig. 9), and very much unlike the Moon or a satellite such as Callisto (see Buratti 1991). Pluto's phase curve thus yields a hint, albeit not very compelling, that Pluto has been recently resurfaced. There is no evidence for an opposition surge on Pluto, although the small excursion in phase angles may mean we are seeing a surge that appears to be linear over the small range observed. This argument has credence because the value of Pluto's phase coefficient is higher than

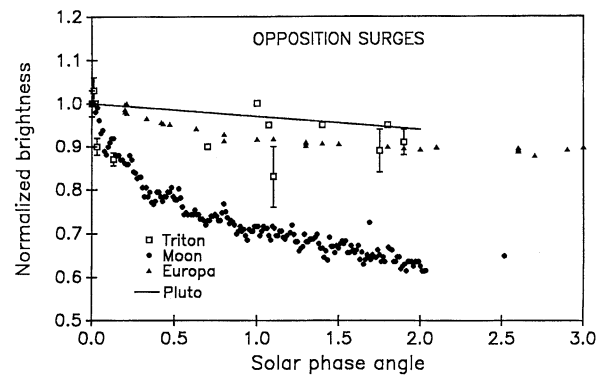


Fig. 9. The phase curve of Pluto–Charon compared with selected bodies in the Solar System. Pluto phase curve is most similar to that of recently resurfaced objects such as Triton and Europa rather than of objects with regoliths that have been formed by meteoritic gardening. The Triton observations are from Goguen et al. (1989), the Europa observations are from Domingue et al. (1991), and the lunar observations are from Buratti et al. (1996).

that of ~ 0.02 typically observed for icy objects with an albedo similar to Pluto's (Buratti and Veverka, 1984). In addition, Pluto may exhibit a narrowly peaked opposition curve at phase angles less than 0.4° . Due to geometrical constraints between the Earth, the Sun, and Pluto, the minimum in Pluto's solar phase angle will not be reached for another 15 years, unless of course a much-needed mission to Pluto is transformed from dream to reality.

Acknowledgments

This work was performed in part at the Jet Propulsion Laboratory, California Institute of Technology, under contract to the National Aeronautics and Space Administration. We thank Dr. Leslie Young and an anonymous reviewer for their detailed and thoughtful reviews. We acknowledge support of NASA's Planetary Geology and Astronomy Programs, and NSF Grant AST 0074555.

References

- Allen, C.W., 1976. *Astrophysical Quantities*. Athlone Press, London.
- Andersson, L.E. 1974. A Photometric study of Pluto and Satellites of the Outer Planets. Ph.D. dissertation, Indiana University.
- Andersson, L.E., Fix, J.P., 1973. Pluto: new photometry and a determination of the axis of rotation. *Icarus* 20, 279–283.
- Binzel, R.P., Mulholland, J.D., 1984. Photometry of Pluto during the 1983 opposition: a new determination of the phase coefficient. *Astron. J.* 89, 1759–1761.
- Blanco, C., DiMartino, M., Ferreri, W., 1994. Observations of Pluto–Charon Mutual Events III. *Astron. J.* 108, 1940–1942.
- Buie, M.W. 2002. Photometry, spectroscopy, and mapping. Talk presented at From here to Pluto–Charon: A New Horizons PKB Mission workshop. Boulder, CO, May 21, 2002.
- Buie, M.W., Fink, U., 1987. Methane absorption in the spectrum of Pluto. *Icarus* 70, 483–498.

- Buie, M.W., Tholen, D.J., Horne, K., 1992. Albedo maps of Pluto and Charon: initial mutual event results. *Icarus* 97, 211–227.
- Buie, M.W., Tholen, D.J., Wasserman, L.H., 1997. Separate lightcurves of Pluto and Charon. *Icarus* 125, 233–244.
- Buratti, B.J., 1984. Voyager disk-resolved photometry of the saturnian satellites. *Icarus* 59, 392–405.
- Buratti, B.J., 1991. Ganymede and Callisto: surface textural dichotomies and photometric analysis. *Icarus* 92, 312–323.
- Buratti, B., Veverka, J., 1983. Voyager photometry of Europa. *Icarus* 55, 93–110.
- Buratti, B., Veverka, J., 1984. Voyager photometry of Rhea, Dione, Tethys, Enceladus, and Mimas. *Icarus* 58, 254–264.
- Buratti, B.J., Goguen, J.D., Gibson, J., Mosher, J., 1994. Historical evidence for volatile migration on Triton. *Icarus* 110, 303–314.
- Buratti, B.J., Hillier, J.K., Wang, M., 1996. The lunar opposition surge: observations by Clementine. *Icarus* 124, 490–499.
- Buratti, B.J., Veverka, J., 1983. Voyager photometry of Europa. *Icarus* 55, 93–110.
- Colina, L., Bohlin, R.C., Castelli, F., 1996. The 0.12–2.5 μm absolute flux distribution of the sun for comparison with solar analog stars. *Astron. J.* 112, 307.
- Cruikshank, D.P., Silvaggio, P.M., 1980. Triton: a satellite with an atmosphere. *Astrophys J.* 233, 1016–1020.
- Cruikshank, D.P., Pilcher, C.B., Morrison, D., 1976. Pluto: evidence for methane frost. *Science* 194, 835–837.
- Davies, J.K., McBride, N., Green, S.F., Mottola, S., Carsenty, U., Basran, D., Hudson, K.A., Foster, M.J., 1998. The lightcurve and colors of unusual minor planet 1996 PW. *Icarus* 132, 418–430.
- Domingue, D.L., Hapke, B.W., Lockwood, G.W., Thompson, D.T., 1991. Europa's phase curve: implications for surface structure. *Icarus* 90, 30–42.
- Doute, S., Schmitt, B., Quirico, E., Cruikshank, D.P., Owen, T.C., deBergh, C., Geballe, T.R., Roush, T.L., 1999. Evidence for methane segregation at the surface of Pluto. *Icarus* 142, 421–444.
- Elliot, J.L., Strobel, D.F., Zhu, X., Stansberry, J.A., Wasserman, L.H., Franz, O.G., 2000. A deep troposphere on Triton. *Icarus* 143, 425–428.
- Goguen, J.D., Hammel, H.B., Brown, R.H., 1989. V photometry of Titania, Oberon, and Triton. *Icarus* 77, 239–247.
- Grundy, W.M., Buie, M.W., 2001. Distribution and evolution of CH_4 , N_2 , and CO ices on Pluto's surface 1995 to 1998. *Icarus* 153, 248–263.
- Grundy, W.M., Fink, U., 1996. Synoptic CCD spectrophotometry of Pluto over the past 15 years. *Icarus* 124, 329–343.
- Hansen, C.J., Paige, D.A., 1996. Seasonal nitrogen cycles on Pluto. *Icarus* 120, 247–265.
- Hapke, B., 1990. Coherent backscatter and the radar characteristics of outer planet satellites. *Icarus* 88, 407–417.
- Horak, H., 1950. Diffuse reflection by planetary atmospheres. *Astrophys. J.* 112, 445–463.
- Hubbard, W.B., Hunten, D.M., Dieters, S.W., Hill, K.M., Watson, R.D., 1989. Occultation evidence for an atmosphere on Pluto. *Nature* 336, 452–454.
- Landolt, A.U., 1992. *UBVRI* photometric standard stars in the magnitude range $11.5 < V < 16.0$ around the celestial equator. *Astron. J.* 104, 340–491.
- Lyutiy, V.M., Tarashchuk, V.P., 1982. A photometric study of Pluto near perihelion. I. U, B, V Photometry. *Sov. Astron. Lett.* 8, 56–59.
- Lyutiy, V.M., Tarashchuk, V.P., 1984. A photometric study of Pluto near perihelion II. Rotation period and color indices. *Sov. Astron. Lett.* 10, 226–229.
- Marcialis, R.L., 1988. A two-spot model for the surface of Pluto. *Astron. J.* 95, 941–947.
- Marcialis, R.L., Lebofsky, L.A., 1991. CVF spectroscopy of Pluto: correlation of composition with albedo. *Icarus* 89, 255–263.
- Marcialis, R.L., Lebofsky, L.A., DiSanti, M.A., Fink, U., Tedesco, E.F., Africano, J., 1993. The albedos of Pluto and Charon: wavelength dependence. *Astron. J.* 103, 1389–1394.
- Millis, R.L., Thompson, D.T., 1975. *UBV* photometry of the Galilean satellites. *Icarus* 26, 408–419.
- Noland, M., Veverka, J., Morrison, D., Cruikshank, D.P., Lazarewicz, A.R., Morrison, N.D., Elliot, J.L., Goguen, J., Burns, J.A., 1974. Six-color photometry of Iapetus, Titan, Rhea, Dione, and Tethys. *Icarus* 23, 334–354.
- Null, G.W., Owen Jr., W.M., Synnott, S.P., 1993. Mass and density of Pluto and Charon. *Astron. J.* 105, 2319–2335.
- Owen, T.C., Roush, T.L., Cruikshank, D.P., Elliot, J.L., Young, L.A., deBergh, C., Schmitt, B., Geballe, T.R., Brown, R.H., Bartholomew, M.J., 1993. Surface ices and atmospheric composition of Pluto. *Science* 261, 745–748.
- Smith, B., Soderblom, L.A., Banfield, D., Barnet, C., Beebe, R.F., Bazi-levskii, A.T., Bollinger, K., Boyce, J.M., Briggs, G.A., Brahic, A., 1989. Imaging science results. *Science* 246, 1422–1449.
- Stansberry, J.A., Yelle, R.V., 1999. Emissivity and the fate of Pluto's atmosphere. *Icarus* 141, 299–306.
- Stansberry, J.A., Lunine, J.I., Hubbard, W.B., Yelle, R.V., Hunten, D.M., 1994. Mirages and the nature of Pluto's atmosphere. *Icarus* 111, 503–513.
- Stansberry, J.A., Spencer, J.R., Schmitt, B., Benchkoura, A., Yelle, R.V., Lunine, J.I., 1996. A model for the overabundance of methane in the atmospheres of Pluto and Triton. *Planet. Space Sci.* 44, 1051–1063.
- Stern, S.A., Trafton, L., 1984. Constraints on bulk composition, seasonal variation, and global dynamics of Pluto's atmosphere. *Icarus* 57, 231–240.
- Stern, S.A., Trafton, L., Gladstone, R., 1988. Why is Pluto bright: implications of the albedo and lightcurve behavior of Pluto. *Icarus* 75, 485–498.
- Stern, S.A., Weintraub, D.A., Festou, M.C., 1993. Evidence for a low surface temperature on Pluto from millimeter wave thermal emission measurements. *Science* 261, 1713–1715.
- Stern, S.A., Buie, M.W., Trafton, L.M., 1997. HST high-resolution images and maps of Pluto. *Astron. J.* 113, 827–843.
- Tholen, D.J., Buie, M., 1997. The orbit of Charon. I. New Hubble Space Telescope observations. *Icarus* 125, 245–260.
- Tholen, D.J., Tedesco, E.F., 1994. Pluto's lightcurve: results from four oppositions. *Icarus* 108, 200–208.
- Trafton, L., 1980. Does Pluto have a substantial atmosphere? *Icarus* 44, 53–61.
- Trafton, L., 1990. A two-component volatile atmosphere for Pluto. I. The bulk hydrodynamic escape regime. *Astrophys J.* 359, 512–523.
- Trafton, L., Stern, S.A., 1983. On the global distribution of Pluto's atmosphere. *Astrophys. J.* 267, 872–881.
- Trafton, L., Matson, D.L., Stansberry, J.A., 1998. Surface/atmosphere interaction and volatile transport (Triton, Pluto and Io), in: Schmitt, B., deBergh, C., Festou, M. (Eds.), *Solar System Ices*, *Astrophys. Space Science Library*, Kluwer Academic, Dordrecht, pp. 773–812.
- Tryka, K.A., Brown, R.H., Cruikshank, D.P., Owen, T.C., Geballe, T.R., deBergh, C., 1994. Temperature of nitrogen ice on Pluto and its implication for flux measurements. *Icarus* 112, 513–527.
- Veverka, J., 1977. Photometry of satellite surfaces, in: Burns, J. (Ed.), *Planetary Satellites*, Univ. of Arizona Press, Tucson, pp. 171–209.
- Whyte, A.J., 1980. *The Planet Pluto*. Pergamon Press, Oxford.
- Young, E.F., Binzel, R.P., 1993. Comparative mapping of Pluto's sub-Charon hemisphere: three least squares models based on mutual event lightcurves. *Icarus* 102, 134–149.
- Young, E.F., Binzel, R.P., 1994. A new determination of radio and limb parameters for Pluto and Charon from mutual event lightcurves. *Icarus* 108, 219–224.
- Young, E.F., Galdamez, K., Buie, M.W., Binzel, R.P., Tholen, D.J., 1999. Mapping the variegated surface of Pluto 1999. *Astron. J.* 117, 1063–1076.
- Young, L. 1994. Bulk properties and atmospheric structure of Pluto and Charon. Ph.D. Dissertation, Massachusetts Institute of Technology, Cambridge.